*Xuzhong Su[1,2],
**Weidong Gao[1,2],
Xinjin Liu[1,2,3],
Chunping Xie[1,2],
Bojun Xu[1,2]

Theoretical Study of the Effects of the General Division of a Ring Spinning Triangle on Fibre Tension

DOI: 10.5604/12303666.1191425

[1]School of Textile and Clothing, Jiangnan University, Wuxi 214122, P. R. China
*E-mail: mfgucv@163.com

[2]Key Laboratory of Eco-Textile, Ministry of Education, Jiangnan University, Wuxi 214122, P. R. China
**E-mail: gaowd3@163

[3]Jiangsu Susi Silk Limited Company, Suqian 223700, P. R. China

Abstract
The geometry of a spinning triangle influences the distribution of fibre tension in it and affects the qualities of spun yarns. Spinning triangle division is one of the most effective measures and fruitful results have been achieved, such as Solospun technology. Therefore a theoretical study of the effects of general ring spinning triangle division on fibre tension is presented in this paper. The general case that the spinning triangle is divided into m parts including m - 1 parts of the primary triangle and one final triangle is investigated and two series of parameters: division proportions β_i and triangle number at each part n_i are introduced for $i = 1, 2, ..., m - 1$. Firstly a theoretical model of the fibre tension distributions at the front roller nip is given by using the principle of minimum potential energy. Secondly numerical simulations of fibre tension distributions in the spinning triangle with different division proportions β_1, β_2 and different numbers of primary triangles n_1, n_2 where $m = 3$ are presented. It is shown that the demarcation of fibre tension between any two adjacent primary triangles in the first part is decreased with an increasein β_1 or β_2 for the fixed n_1 and n_2. Meanwhile, for the fixed β_1 and β_2, the total magnitude of fibre tension is increased greatly with an decrease in n_1, whereas it rises slightly with an increase in n_2. Finally the effects of spinning triangle division on yarn qualities are analysed according to the numerical simulations and previous results.

Key words: *general division of spinning triangles, fibre tension, ring spinning.*

Introduction

During the ring spinning process, the fibre strand comes from the draft zone firstly, which is flat and parallel to the twisting axis of the strand at this time. Then the fibre strands rotate around the axis and the width begins to decrease with the twisting, and the fibres on both sides of the axis fold gradually and roll into the centre of the spun yarn, with the spinning triangle forming simultaneously [1]. Therefore the spinning triangle is a critical region in the spinning process, whose geometry influences the fibre tension distribution in it and affects the properties of spun yarn [2 - 4]. Taking appropriate measures to influence the ring spinning triangle geometry and improve the quality of yarn has attracted great interest recently [5, 6], such as the Sirospun [7], Solospun [8], and Compact spinning technologies [9]. As is known, spinning triangle division is one of the most effective measures, and fruitful results have been achieved, such as Solospun technology, which is implemented by dividing one ring spinning triangle into several small primary triangles and one final triangle using a Solospun roller [8]. Therefore the effects of ring spinning triangle division on fibre tension are theoretically studied in this paper. The general case that the spinning triangle is divided into *m* parts including *m* - 1 parts of the primary triangle and one final triangle is investigated.

The subject of the spinning triangle has been one of the most important research topics and has attracted more and more attention recently, with a lot of results having been achieved [2 - 4, 10, 11]. The force balance of fibres on the spinning triangle was first considered in theory by studying the twist irregularity of cotton and worsted spun yarns in ring spinning [10]. Then in order to predict the fibre tension distribution in the spinning triangle and study the effects of spinning triangle geometry on yarn qualities, a theoretical model of fibre tension distribution in a a symmetric spinning triangle was developed by using the principle of stationary total potential energy [11]. However, the spinning triangles are often asymmetric due to the frictional contact of fibres with the bottom roller in some real situations, and this model was further extended to this kind of asymmetric spinning triangle by introducing a shape parameter for describing the skew level of the spinning triangle geometry [2]. Then the effects of the horizontal offset of the ring spinning triangle on yarn qualities was investigated [19], and corresponding yarn torque caused by fibre tension in the spinning triangle was discussed theoretically [20]. Moreover

spinning triangles are also asymmetric due to the horizontal offset between the twisting point and the symmetric axis of the nip line at the spinning triangle in some modified ring spinning systems, i.e. yarn spinning tension has an obvious angle, with the vertical axis perpendicular to the nip line [5, 6], and a model was further proposed for this situation [4]. Furthermore quantitative relationships between the mechanical performance of the ring spinning triangle and spinning parameters were investigated by using the Finite Element Method (FEM) [12].

Motivated by all the research works above, this paper attempts to investigate the effect of ring spinning triangle division on fibre tension distribution in a general case, that is, the spinning triangle is divided into m parts including m - 1 parts of the primary triangle, and one final triangle is investigated. Two series of parameters: division proportions β_i and the primary triangle number at each part n_i are introduced for i = 2, ..., m. Theoretical models of the fibre tension distributions on one final and m - 1 parts of the primary spinning triangles are given, respectively, by using the principle of minimum potential energy. With the help of a high-speed camera, the fibre tension distributions on spinning triangles with

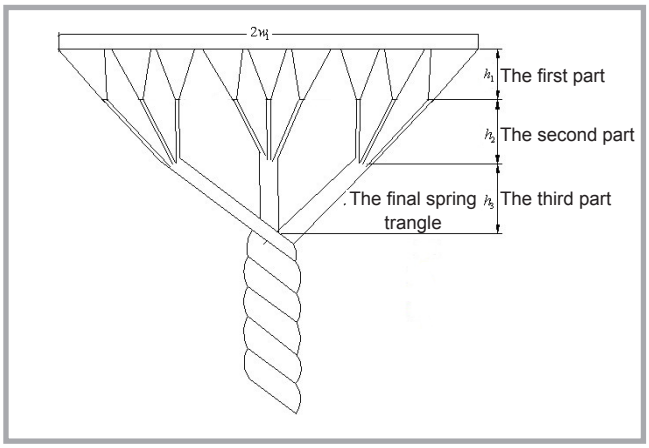

Figure 1. *Divided Spinning triangle model, where m = 3.*

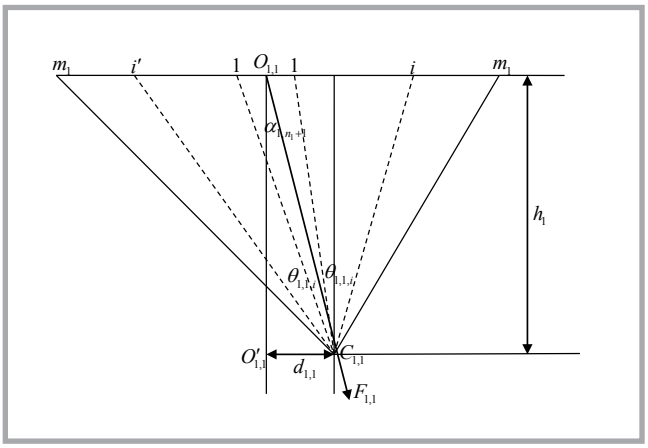

Figure 2. *Fibre distribution on the left boundary primary spinning triangle of the first part.*

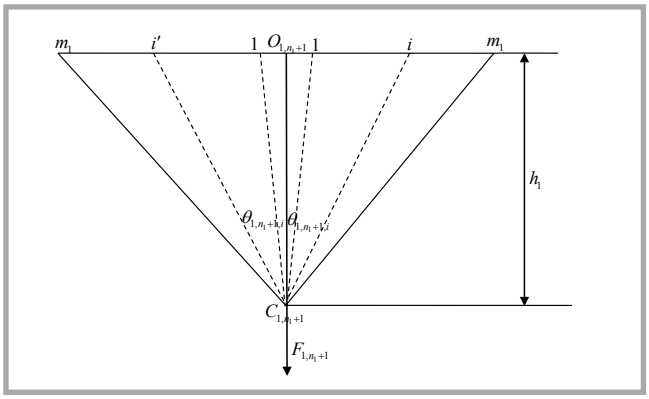

Figure 3. *Fibre distribution on the middle primary spinning triangle of the first part.*

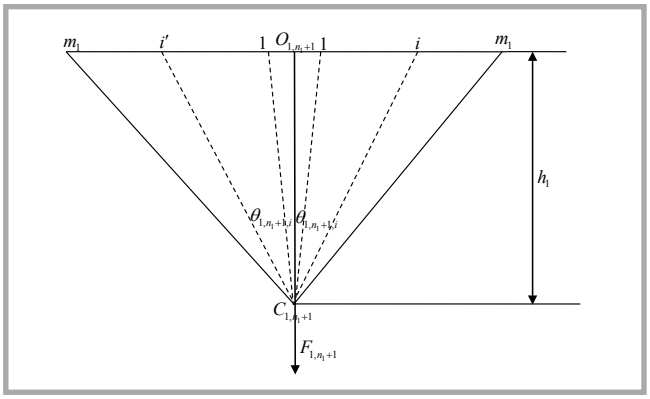

Figure 4. *Fibre distribution on the right boundary primary spinning triangle of the first part.*

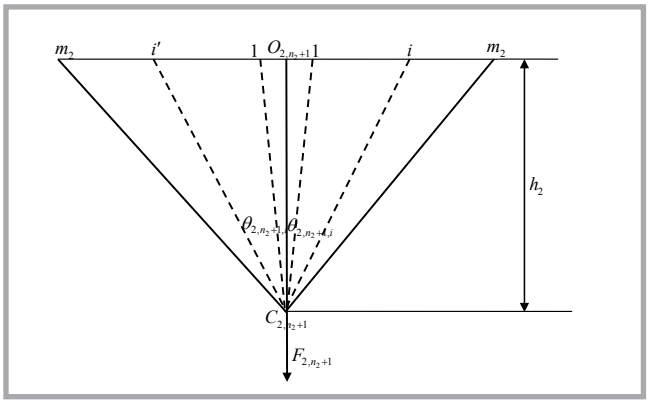

Figure 5. *Substrand distribution in the middle primary spinning triangle of the second part.*

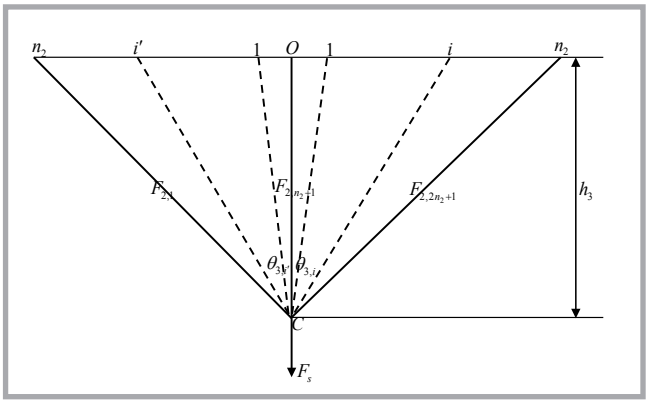

Figure 6. *Substrand distribution in the final spinning triangle.*

different division proportions and different primary triangle numbers on each part are simulated numerically.

Theoretical analysis

The divided spinning triangle model is shown in ***Figure 1*** where $m = 3$. Here, h_3 is the height of the final triangle, h_1 and h_2 the height of primary spinning triangles in the two divided parts, respectively, $H = h_1 + h_2 + h_3$ the height of the ring spinning triangle, and $\beta_1 = h_1/H$ & $\beta_2 = h_2/H$ are defined as the division proportions, resulting in $h_1/H = 1 - \beta_1 - \beta_2$. Suppose that the total number of fibres in all primary triangles in the first divided part is $2n + 1$, and the total number of substrands in the second divided part and the final triangle is $2n_1 + 1$ and $2n_2 + 1$, respectively, then it is obvious that the number of primary triangles in the first and second parts is equal to $2n_1 + 1$ and $2n_2 + 1$, respectively, and we get $2s_1 + 1 = (2n + 1)/(2n_1 + 1)$, denoting the number of fibres in each primary triangle in the first part, and $2s_2 + 1 = (2n_1 + 1)/(2n_2 + 1)$, denoting the number of substrands in each primary triangle in the second part. Three primary spinning triangle models in the first part including the left and right boundary and middle triangles are shown in ***Figures 2*** & ***4*** respectively. Here, $O_{1,j}$ is the middle point of each primary triangle at the front roller nip line, $C_{1,j}$ the twisting point with load $F_{1,j}$; the direction of $F_{1,j}$ is assumed to act along the line $O_{1,j}C_{1,j}$; $\alpha_{1,j}$ is the inclination angle of the spinning tension, $\theta_{1,j,i}$ the angle between the right i-th fibre and central fibre, and $\theta_{1,j,i'}$ is the angle between the left i'-th fibre and the central fibre, respectively, for j = 1, 2, ..., $2n_1 + 1$. The middle primary spinning triangle model in the second part is shown in ***Figure 5***. The final spinning triangle model is shown in ***Figure 6***. Here, O is the middle point at the nip line, C the twisting point with constant load F_s, $\theta_{3,i}$ the angle between the right i-th fibre and central fibre, and $\theta_{3,i'}$ the angle between the left i'-th fibre and central fibre, respectively. Suppose that the half width of the ring spinning triangle at the front roller nip line is w_1.

According to ***Figures 2 - 6***, we have

$$\begin{aligned}\alpha_{1,j'+(k-1)(2s_2+1)} &= \theta_{2,k,j'} + \alpha_{2,k}\,,\\ \alpha_{1,j+(k-1)(2s_2+1)+s_2} &= \theta_{2,k,j} - \alpha_{2,k}\end{aligned} \tag{1}$$

where, $j', j = 1, 2, \cdots, s_2 + 1$,

$$k = 1, 2, \cdots, n_1 + 1\,.$$

$$\alpha_{2,j} = \theta_{3,j}\,,\ \alpha_{2,j'} = \theta_{3,j'} \tag{2}$$

Where $j', j = 1, 2, \cdots, n_2 + 1$.

$$\begin{aligned}w_2 &= \frac{h_2 + h_3}{H} w_1 = (1 - \beta_1) w_1\,,\\ w_3 &= \frac{h_3}{H} w_1 = (1 - \beta_1 - \beta_2) w_1\end{aligned} \tag{3}$$

Where w_2 denotes the half width of all primary spinning triangles in the second part, and w_3 the half width of the final spinning triangle.

For convenience of analysis, we make the following assumptions [4]: the cross-section of all fibres is a circle with identical diameters; all fibres are gripped between the front roller nip and convergence point; fibre slippage and migration and frictional contact between fibres and the front roller is taken into consideration; the velocity of fibres in the spinning triangle is constant; fibre stress-strain behaviour follows Hook's law for small strain, and the ends of all fibres gripped in the front roller nip distribute evenly.

In the following section, a general case where the spinning triangle is divided into m parts including m - 1 parts of the primary triangle and one final triangle will be investigated. Fibre tension distributions in the primary triangles in the first part and the substrand tension distributions on the primary spinning triangle in the other part will be analyzed using the principle of minimum potential energy, respectively. According to the analysis above, for obtaining the fibre tension distribution at the front roller nip line, i.e. fibre tension in the primary spinning triangles in the first part, the substrand tension in the final spinning triangle should be given firstly, and the substrand tension in the primary spinning triangles in the m - 1th, m - 2th, ..., 2nd part will be given successively. Fibre tension distributions in all the primary spinning triangles in the first part can be calculated as the following steps.

Step 1: By using the principle of minimum potential energy, the substrand tension distribution in the final triangle can be expressed as show in ***Equation 4*** (see end of column 3), where, $2n_{m-1} + 1$ denotes the number of substrands in the final spinning triangle, $2v_{m-1} + 1 = \dfrac{2n+1}{2n_{m-1}+1}$ the number of fibres in each substrand, A the cross-section of fibre, E the fibre tensile Young's modulus, $M_{m,j} = \dfrac{1}{\cos\theta_{m,j}}$, $M_{m,j'} = \dfrac{1}{\cos\theta_{m,j'}}$, $\tan\theta_{m,j} = \tan\theta_{m,j'} = j\dfrac{w_m}{n_{m-1}h_m}$, $w_m = \dfrac{h_m}{H} w_1 = \left(1 - \sum_{i=1}^{m-1}\beta_i\right) w_1$ the half width of the final spinning triangle, $\beta_i = \dfrac{h_i}{H}$ the division proportions, and h_i is the height of the primary spinning triangles at the i-th part for i = 1, 2, ..., m - 1.

Step 2: According to the analysis above, the substrand tension in the primary triangles in the m - 1th part can be given as shown in ***Equation 5***, where, $2s_{m-1} + 1 = \dfrac{2n_{m-2}+1}{2n_{m-1}+1}$ denotes the number of substrands on each primary spinning triangle, and $2v_{m-2} + 1 = \dfrac{2n+1}{2n_{m-2}+1}$ the number of fibres in each substrand (see ***Equation 6***, page 40).

Step 3: In the general case, the substrand tension in the primary triangles in the k-th part can be given as shown in

$$F_{m,j=0,1,\cdots,n_{m-1}} = \frac{F_s - 2(2v_{m-1}+1)AE\sum_{j=1}^{n_{m-1}} M_{m,j}(M_{m,j}-1)}{2\sum_{j=1}^{n} M_{m,j}{}^2 - 1} M_{m,j} + (2v_{m-1}+1)AE(M_{m,j}-1)$$

$$F_{m,j'=0,1,\cdots,n_{m-1}} = \frac{F_s - 2(2v_{m-1}+1)AE\sum_{j'=1}^{n_{m-1}} M_{m,j'}(M_{m,j'}-1)}{2\sum_{j'=1}^{m} M_{m,j'}{}^2 - 1} M_{m,j'} + (2v_{m-1}+1)AE(M_{m,j'}-1) \tag{4}$$

$$\begin{aligned}F_{m-1,j=0,1,\cdots,n_{m-1},i=0,1,\cdots,s_{m-1}} &= \Gamma_{m-1,j} M_{m-1,j,i} + (2v_{m-2}+1)AE(M_{m-1,j,i}-1)\\ F_{m-1,j=0,1,\cdots,n_{m-1},i'=0,1,\cdots,s_{m-1}} &= \Gamma_{m-1,j} M_{m-1,j,i'} + (2v_{m-2}+1)AE(M_{m-1,j,i'}-1)\end{aligned} \tag{5}$$

Equation 4.

$$\Gamma_{m-1,j}=\frac{F_{m,j}-(2v_{m-2}+1)AE\left(\sum_{i=1}^{s_{m-1}}M_{m-1,j,i}\left(M_{m-1,j,i}-1\right)+\sum_{i'=1}^{s_{m-1}}M_{m-1,j,i'}\left(M_{m-1,j,i'}-1\right)\right)}{\sum_{i=1}^{s_{m-1}}M_{m-1,j,i}{}^{2}+\sum_{i'=1}^{s_{m-1}}M_{m-1,j,i'}{}^{2}-1}$$

$$M_{m-1,j,i}=\frac{1}{\cos\theta_{m-1,j,i}-\tan\alpha_{m,j}\sin\theta_{m-1,j,i}} \qquad w_{m-1,i}=i\frac{w_{m-1}}{n_{m-2}} \tag{6}$$

$$M_{m-1,j,i'}=\frac{1}{\cos\theta_{m-1,j,i'}+\tan\alpha_{m,j}\sin\theta_{m-1,j,i'}} \qquad w_{m-1,i'}=i'\frac{w_{m-1}}{n_{m-2}} \qquad \alpha_{m,j}=\theta_{m,j}$$

$$\tan\left(\theta_{m-1,j,i'}-\alpha_{m,j}\right)=\frac{w_{m-1,i'}-h_{m-1}\tan\theta_{m,j}}{h_{m-1}} \qquad w_{m-1}=\frac{h_m+h_{m-1}}{H}w_1=\left(1-\sum_{i=1}^{m-2}\beta_i\right)w_1$$

$$F_{m-1,j'=0,1,\cdots,n_{m-1},i=0,1,\cdots,s_{m-1}}=\Gamma_{m-1,j'}M_{m-1,j',i}+(2v_{m-2}+1)AE\left(M_{m-1,j',i}-1\right)$$

$$F_{m-1,j'=0,1,\cdots,n_{m-1},i'=0,1,\cdots,s_{m-1}}=\Gamma_{m-1,j'}M_{m-1,j',i'}+(2v_{m-2}+1)AE\left(M_{m-1,j',i'}-1\right)$$

where,

$$\Gamma_{m-1,j'}=\frac{F_{m,j'}-(2v_{m-2}+1)AE\left(\sum_{i=1}^{s_{m-1}}M_{m-1,j',i}\left(M_{m-1,j',i}-1\right)+\sum_{i'=1}^{s_{m-1}}M_{m-1,j',i'}\left(M_{m-1,j',i'}-1\right)\right)}{\sum_{i=1}^{s_{m-1}}M_{m-1,j',i}{}^{2}+\sum_{i'=1}^{s_{m-1}}M_{m-1,j',i'}{}^{2}-1}$$

$$M_{m-1,j',i}=\frac{1}{\cos\theta_{m-1,j',i}+\tan\alpha_{m,j'}\sin\theta_{m-1,j',i}}$$

$$M_{m-1,j',i'}=\frac{1}{\cos\theta_{m-1,j',i'}-\tan\alpha_{m,j'}\sin\theta_{m-1,j',i'}}$$

$$\tan\left(\theta_{m-1,j',i'}+\alpha_{m,j'}\right)=\frac{w_{m-1,i'}+h_{m-1}\tan\theta_{m,j'}}{h_{m-1}}$$

$$\tan\left(\theta_{m-1,j',i}-\alpha_{m,j'}\right)=\frac{w_{m-1,i}-h_{m-1}\tan\theta_{m,j'}}{h_{m-1}} \qquad \alpha_{m,j'}=\theta_{m,j'}$$

$$F_{k,j=0,1,\cdots,n_k,i=0,1,\cdots,s_k}=\Gamma_{k,j}M_{k,j,i}+(2v_{k-1}+1)AE\left(M_{k,j,i}-1\right)$$
$$F_{k,j=0,1,\cdots,n_k,i'=0,1,\cdots,s_k}=\Gamma_{k,j}M_{k,j,i'}+(2v_{k-1}+1)AE\left(M_{k,j,i'}-1\right) \tag{7}$$

Equations 6 and 7.

Equation 7, where, $2s_k+1=\frac{2n_{k-1}+1}{2n_k+1}$ denotes the substrand number on each primary spinning triangle, and $2v_{k-1}+1=\frac{2n+1}{2n_{k-1}+1}$ the total fibre number in each substrand (see ***Equation 8***, page 41).

Step 4: Finally fibre tension in the primary spinning triangles in the first part can be given as shown ***Equations 9*** & ***10*** (see page 41).

Simulations and discussions

From ***Equations 4 - 10***, it is obvious that the fibre tension distribution in the spinning triangle mainly depends on the spinning tension, the number of divided parts, the number of primary triangles in each part, the division proportions, the fibre tensile Young's modulus and cross-section, and the height and width of the ring spinning triangle. To obtain the height of the ring spinning triangle, a high speed camera should be applied. In the experiment, a high speed camera system OLYMPUS i-speed3 was set up above the transparent roller and used to capture the geometry of the ring spinning triangle. The yarn and fibre parameters of 184.5 dtex cotton yarn used in the analysis are as follows: $w_1 = 1.65$ mm, $H = 2.9$ mm, yarn spinning tension F_s = 20 cN, fibre Young's modulus E = 50 cN/tex, number of fibres in the yarn $2n + 1 = 135$, fibre linear density $A = 0.15$ tex, the number of divided parts $m = 3$, and the twist direction "Z". By using Matlab software, numerical simulation results of the fibre tension distributions in the spinning triangle with different division proportions β_1, β_2 and different numbers of primary triangles n_1, n_2 were obtained, shown in ***Figure 7*** respectively. Here, the x-axis denotes the serial number of the fibres at the front roller nip from left to right, the y-axis -the fibre tension, and the negative value indicates the compressive force, whereas the positive value indicates the tensile force.

In this paper, the symmetrical spinning triangle is considered only, thus the distributions of fibre tension are symmetrical about the central fibre in all simulations. The asymmetrical spinning triangle, due to the frictional contact of fibres with the bottom roller [2] or the angle with the vertical axis perpendicular to the nip line [4], can also be considered similarly. Fibre tension distribution in spinning triangles with five different division proportions β_1, where $\beta_2 = 0.5$, $n_1 = 7$ and $n_2 = 1$, is shown in ***Figure 7a***. Here, $\beta_1 = 0$ denotes the spinning triangle without division. It is shown that the demarcation of fibre tension in the fifteen primary triangles in the first part decreases with an increase in β_1, i.e. the curve becomes more and more smooth, and the total magnitudes of fibre tension also decreases slightly. One possible explanation is that with an increase in β_1, the height h_1 increases, and the angle between the left boundary fibre in the j-th primary triangle and the right boundary fibre in the $j + 1$-th primary triangle decreases by $j = 1, 2, ..., 2n_1$, which leads to the less demarcation of fibre tension between the two adjacent primary triangles. Fibre tension distribution in the spinning triangles with five different division proportions β_2, where $\beta_1 = 0.5$, $n_1 = 7$ and $n_2 = 1$ is shown in ***Figure 7.b***. It is also exhibited that the demarcation of fibre tension in the fifteen primary triangles in the first part decreases with an increase in β_2, and the total magnitudes of fibre tension decreases slightly. Meanwhile, comparing with ***Figure 7.a***, the fluctuation of fibre tension is more obvious.

To analyse the effects of the primary triangle number in the first part n_1 on fibre tension, numerical simulations with another two values $n_1 = 13$ and $n_1 = 3$ are given in ***Figures 7.c - 7.f***. Comparing with the situation $n_1 = 7$ in ***Fig-***

ures 7.a - 7.b, it is shown that the tendency of the fibre tension distribution curve is consistent in all three cases. However, the total magnitudes of fibre tension increase greatly with a decrease in n_1. Similarly, to analyse the effects of the primary triangle number in the second part n_2 on fibre tension, numerical simulations with another value $n_2 = 4$ are given in ***Figures 7.g - 7.h*** where $n_1 = 13$. Comparing with the situation $n_2 = 1$ in ***Figures 7.c - 7.d***, it is also shown that the tendency of the fibre tension distribution curve is consistent in both two cases. However, the total magnitudes of fibre tension increase slightly and the fluctuation of the curve decreases slightly with an increase in n_2.

As is known, spinning triangle division is one of the most effective measures to influence ring spinning triangle geometry and improve the quality of yarn, and fruitful results have been achieved, such as Solospun technology, which is implemented by dividing one ring spinning triangle into several small primary triangles and one final triangle using a Solospun roller [8]. That is, the spinning triangle is divided into two parts: primary triangles and the final triangle in Solospun technology. The advantages of Solospun spinning have been shown comparing to ring spinning [13], such as less hairiness, which further confirms the positive effect of spinning division on improving yarn qualities. Therefore, in this paper, a theoretical study of the effects of Ring spinning triangle division on fibre tension is presented, and the general case that the spinning triangle is divided into m parts including m - 1 parts of primary triangles and one final triangle has been investigated. Theoretical models of the fibre tension distributions at the front roller nip have been presented using the principle of minimum potential energy, which lays a theoretical foundation for new spinning technology.

Yarn torque is one of the important indexes of yarn quality, which is determined on the basis of fibre tension translation in the spinning triangle [14]. It has been shown that the fibre tension within a yarn was the most significant factor contributing to yarn torque, and smaller fibre tension magnitude can produce lower yarn torque [4]. According to the numerical simulation results above, the magnitudes of fibre tension can be decreased by using appropriate spinning triangle division. Hairiness is another of the most

$$\Gamma_{k,j}=\frac{F_{k+1,j}-\left(2v_{k-2}+1\right)AE\left(\sum_{i=1}^{s_k}M_{k,j,i}\left(M_{k,j,i}-1\right)+\sum_{i'=1}^{s_k}M_{k,j,i'}\left(M_{k,j,i'}-1\right)\right)}{\sum_{i=1}^{s_k}{M_{k,j,i}}^2+\sum_{i'=1}^{s_k}{M_{k,j,i'}}^2-1} \tag{8}$$

$$M_{k,j,i}=\frac{1}{\cos\theta_{k,j,i}-\tan\alpha_{k,j}\sin\theta_{k,j,i}} \qquad M_{k,j,i'}=\frac{1}{\cos\theta_{k,j,i'}+\tan\alpha_{k,j}\sin\theta_{k,j,i'}}$$

$$\tan\left(\theta_{k,j,i'}-\alpha_{k,j}\right)=\frac{w_{k,i'}-h_k\tan\alpha_{k,j}}{h_k} \qquad \tan\left(\theta_{k,j,i}+\alpha_{k,j}\right)=\frac{w_{k,i}+h_k\tan\alpha_{k,j}}{h_k}$$

$$w_{k,i'}=i'\frac{w_k}{n_{k-1}} \qquad w_{k,i}=i\frac{w_k}{n_{k-1}} \qquad w_k=\frac{\sum_{i=k}^{m}h_i}{H}w_1=\left(1-\sum_{i=1}^{k-1}\beta_i\right)w_1$$

$$F_{k+1,j}=\begin{cases}F_{k+1,t'+l(2s_{k+1}+1)}=F_{k+1,l,t'}\\F_{k+1,t+l(2s_{k+1}+1)+s_{k+1}}=F_{k+1,l,t}\end{cases} \qquad \alpha_{k,t'+(l-1)(2s_k+1)}=\theta_{k+1,l,t'}+\alpha_{k+1,l} \qquad \text{and}$$

$$\alpha_{k,t+(l-1)(2s_k+1)}=\alpha_{k+1,l}-\theta_{k+1,l,t} \qquad \text{for} \quad t,t'=0,1,\cdots,s_{k+1} \quad \text{and} \quad l=0,1,\cdots,n_{k+1}$$

$$F_{k,j'=0,1,\cdots,n_k,i=0,1,\cdots,s_k}=\Gamma_{k,j'}M_{k,j',i}+\left(2v_{k-1}+1\right)AE\left(M_{k,j',i}-1\right)$$

$$F_{k,j'=0,1,\cdots,n_k,i'=0,1,\cdots,s_k}=\Gamma_{k,j'}M_{k,j',i'}+\left(2v_{k-1}+1\right)AE\left(M_{k,j',i'}-1\right)$$

where,

$$\Gamma_{k,j'}=\frac{F_{k+1,j'}-\left(2v_{k-2}+1\right)AE\left(\sum_{i=1}^{s_k}M_{k,j',i}\left(M_{k,j',i}-1\right)+\sum_{i'=1}^{s_k}M_{k,j',i'}\left(M_{k,j',i'}-1\right)\right)}{\sum_{i=1}^{s_k}{M_{k,j',i}}^2+\sum_{i'=1}^{s_k}{M_{k,j',i'}}^2-1}$$

$$F_{k+1,j'}=\begin{cases}F_{k+1,t'+l'(2s_{k+1}+1)}=F_{k+1,l',t'}\\F_{k+1,t+l'(2s_{k+1}+1)+s_{k+1}}=F_{k+1,l',t}\end{cases} \quad \text{for} \quad t,t'=0,1,\cdots,s_{k+1} \quad \text{and} \quad l'=0,1,\cdots,n_{k+1}$$

$$M_{k,j',i}=\frac{1}{\cos\theta_{k,j',i}+\tan\alpha_{k,j'}\sin\theta_{k,j',i}} \qquad M_{k,j',i'}=\frac{1}{\cos\theta_{k,j',i'}-\tan\alpha_{k,j'}\sin\theta_{k,j',i'}}$$

$$\tan\left(\theta_{k,j',i'}+\alpha_{k,j'}\right)=\frac{w_{k,i'}+h_k\tan\alpha_{k,j}}{h_k} \qquad \tan\left(\theta_{k,j,i}-\alpha_{k,j}\right)=\frac{w_{k,i}-h_k\tan\alpha_{k,j'}}{h_k}$$

$$\alpha_{k,j'}=\alpha_{k,j}$$

$$\begin{aligned}&F_{1,j=0,1,\cdots,n_1,i=0,1,\cdots,s_1}=\Gamma_{1,j}M_{1,j,i}+AE\left(M_{1,j,i}-1\right)\\&F_{1,j=0,1,\cdots,n_1,i'=0,1,\cdots,s_1}=\Gamma_{1,j}M_{1,j,i'}+AE\left(M_{1,j,i'}-1\right)\end{aligned} \tag{9}$$

$$\begin{aligned}&F_{1,j'=0,1,\cdots,n_1,i=0,1,\cdots,s_1}=\Gamma_{1,j'}M_{1,j',i}+AE\left(M_{1,j',i}-1\right)\\&F_{1,j'=0,1,\cdots,n_1,i'=0,1,\cdots,s_1}=\Gamma_{1,j'}M_{1,j',i'}+AE\left(M_{1,j',i'}-1\right)\end{aligned} \tag{10}$$

here,

$$\Gamma_{1,j}=\frac{F_{2,j}-AE\left(\sum_{i=1}^{s_1}M_{1,j,i}\left(M_{1,j,i}-1\right)+\sum_{i'=1}^{s_1}M_{1,j,i'}\left(M_{1,j,i'}-1\right)\right)}{\sum_{i=1}^{s_1}{M_{1,j,i}}^2+\sum_{i'=1}^{s_1}{M_{1,j,i'}}^2-1}$$

$$\Gamma_{1,j'}=\frac{F_{2,j'}-AE\left(\sum_{i=1}^{s_1}M_{1,j',i}\left(M_{1,j',i}-1\right)+\sum_{i'=1}^{s_1}M_{1,j',i'}\left(M_{1,j',i'}-1\right)\right)}{\sum_{i=1}^{s_1}{M_{1,j',i}}^2+\sum_{i'=1}^{s_1}{M_{1,j',i'}}^2-1}$$

Equations 8, 9 and 10.

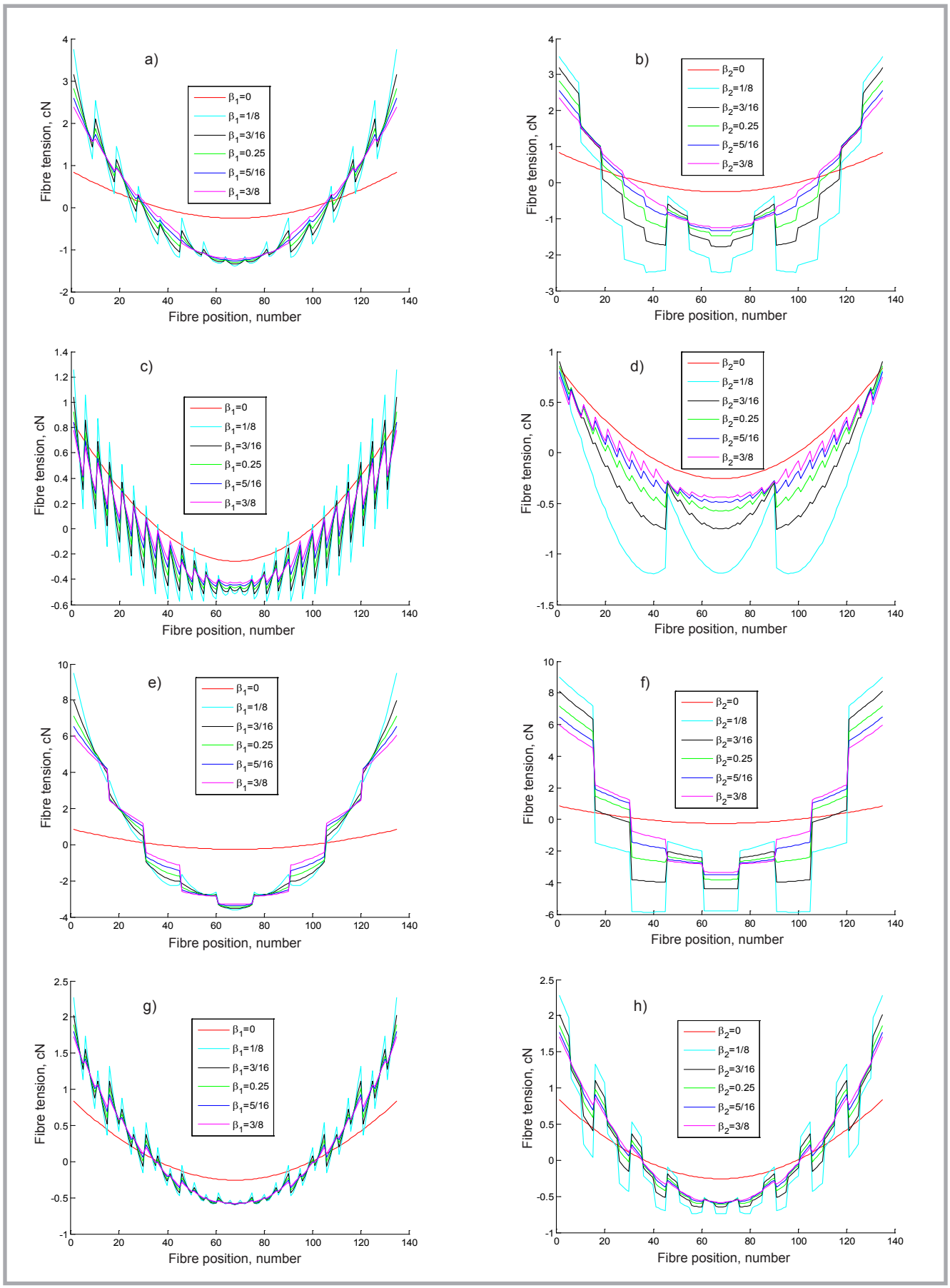

Figure 7. *Fibre tension distribution in the spinning triangles with different division proportions: a) β_1, where $n_1 = 7$, $n_2 = 1$ and $\beta_2 = 0.5$; b) β_2, where $n_1 = 7$, $n_2 = 1$ and $\beta_1 = 0.5$; c) β_1, where $n_1 = 13$, $n_2 = 1$ and $\beta_2 = 0.5$; d) β_2, where $n_1 = 13$, $n_2 = 1$ and $\beta_1 = 0.5$; e) β_1, where $n_1 = 7$, $n_2 = 1$ and $\beta_2 = 0.5$; f) β_2, where $n_1 = 3$, $n_2 = 1$ and $\beta_1 = 0.5$; g) β_1, where $n_1 = 13$, $n_2 = 4$ and $\beta_2 = 0.5$; h) β_2, where $n_1 = 13$, $n_2 = 4$ and $\beta_1 = 0.5$.*

important properties of spun yarn. It has been shown that larger tension forces acting on the outer fibres of the spinning triangle would reduce yarn hairiness [15 - 17]. According to the numerical simulation results above, the tension of outer fibres at the front roller nip can be obviously increased with appropriate spinning triangle division. Meanwhile lots of hairiness will be rolled into the spun yarn body when the substrands are twisted into yarn on the final spinning triangle under twisting [8]. Therefore appropriate Ring spinning triangle division would be beneficial for yarn hairiness reduction. Yarn strength is another property of great concern in evaluating yarn performance, which can be reinforced by increasing the lateral pressure between fibres [18]. The fibre number in each primary spinning triangle decreases with an increase in the spinning triangle division, which can help to transfer the twist uniformly, which is beneficial for tension balance on the spinning triangle. Then the lateral pressure between fibres can be increased.

Conclusions

In this paper, the effects of general Ring spinning triangle division on fibre tension distribution have been studied theoretically. The general case that the spinning triangle is divided into m parts including m - 1 parts of the primary triangle and one final triangle has been investigated, with two series of parameters: division proportions β_i, which described the ratio of each divided part's height to the total spinning triangle height and the primary triangle number in each part n_i for $i = 1, 2, ..., m - 1$, being introduced in the analysis. The analysis indicated that the individual fibre tension in the divided spinning triangle can be determined by the spinning tension, the number of divided parts, the number of primary triangles in each part, the division proportions, the fibre tensile Young's modulus and cross-section, and the height and width of the ring spinning triangle.

The numerical simulation results for 184.5 dtex cotton yarn have been presented using Matlab software according to the theoretical models proposed, where $m = 3$. The fibre tension distributions in the spinning triangle with different division proportions β_1, β_2 and different numbers of primary triangles in two parts n_1, n_2 have been presented. It is shown that the demarcation of fibre tension in the primary triangles in the first part decreases with an increase in β_1 or β_2, i.e. the curve becomes more and more smooth, and the total magnitudes of fibre tension also decreases slightly. Meanwhile the total magnitudes of fibre tension increase greatly with an decrease in n_1 but rise slightly with an increase in n_2. Finally, according to the numerical simulations and previous results, the effects of ring spinning triangle division on yarn qualities have been analysed. It is shown that appropriate Ring spinning triangle division would be beneficial for improving yarn quality. Therefore the theoretical model given in this paper lays the foundation for spinning technology innovation.

Acknowledgements

This work was supported by the National Natural Science Foundation of P. R. China under Grant 11102072, the Natural Science Foundation of Jiangsu Province under Grant (BK20151359), Prospective industry-university-research project of Jiangsu Province (BY2014023-13, BY2015019-10), Prospective industry-university-research project of Guangdong Province (2013B090600038), Henan collaborative innovation of textile and clothing industry (hnfz14002).

Reference

1. Przybyl K. Simulating the dynamics of the twisting-and-winding system of the ring spinning frame. *Fibres and Textiles in Eastern Europe* 2001; 9, 1(32): 16-19.
2. Hua T, Tao X M, Cheng KPS, Xu BG. Effects of Geometry of Ring Spinning Triangle on Yarn Torque Part I: Analysis of Fiber Tension Distribution. *Textile Research Journal* 2007; 77, 11: 853-863.
3. Hua T, Tao X M, Cheng KPS, Xu BG. Effects of Geometry of Ring Spinning Triangle on Yarn Torque: Part II: Distribution of Fiber Tension within a Yarn and Its Effects on Yarn Residual Torque. *Textile Research Journal* 2010; 80, 2: 116-123.
4. Feng J, Xu BG, Tao XM, Hua T. Theoretical Study of Spinning Triangle with Its Application in a Modified Ring Spinning System. *Textile Research Journal* 2010; 80, 14: 1456-1464.
5. Wang XG, Chang LL. Reducing Yarn Hairiness with a Modified Yarn Path in Worsted Ring Spinning. *Research Journal of Textile and Apparel* 2003; 73, 4: 327- 332.
6. Thilagavathi G, Udayakumar D, Sasikala L. Yarn hairiness controlled by various left diagonal yarn path offsets by modified bottom roller flute blocks in ring spinning. *Indian Journal of Fiber and Textile Research* 2009; 34: 328-332.
7. An XL, Yu CW. Dynamic model of sirospun process. Part I: theoretical dynamic model. *Journal of the Textile Institute* 2010; 101, 9:805-811.
8. Cheng LD, Fu PH, Yu XY. Relationship between hairiness and the twisting principles of solospun and ring spun yarns. *Textile Research Journal* 2004; 74, 9: 763- 766.
9. Momir N, Zoran S, Franc L, Andrej S. Compact Spinning for Improved Quality of Ring-Spun Yarns. *Fibers & Textiles in Eastern Europe* 2003; 11, 4: 30-35.
10. Fujino K, Uno M, Shiomi A, Yanagawa Y, Kitada Y. A Study on the Twist Irregularity of Yarns Spun on the Ring Spinning Frame. *The Textile Machinery Society of Japan* 1962; 8: 51-62.
11. Shaikhzadeh NS. An Analysis of the Twist Triangle in Ring Spinning. PhD Thesis, University of New South Wales, Australia, 1996.
12. Li SY, Xu BG, Tao M X. Numerical Analysis on Mechanical Behavior of a Ring-Spinning Triangle Using the Finite Element Method. *Textile Research Journal* 2011: 81, 9: 959-971.
13. Chang LL, Wang XG. Comparing the hairiness of Solospun and ring spun worsted yarns. *Textile Research Journal* 2003; 73, 7: 640-644.
14. Bennett JM and Postle R. A Study of Yarn Torque and Its Dependence on the Distribution of Fiber Tension in the Yarn, Part I: Theoretical Analysis, Part II: Experimental. *Journal of the Textile Institute* 1979; 70, 4: 121-141.
15. Beltran Rafael, Wang LJ, Wang XG. A Controlled Experimental on Yarn Hairiness and Fabric Pilling. *Journal of Textile Research* 2007; 77, 3: 179-183.
16. Cheng KPS, Li CHL. JetRing Spinning and its Influence on Yarn Hairiness. *Journal of Textile Research* 2002; 72, 1079-1087.
17. Kalyanaraman AR. A Process to Control Hairiness in Yarn. *Journal of the Textile Institute* 1992; 83, 3:407-413.
18. Yang K, Tao XM, Xu BG, Jimmy L. Structure and Properties of Low Twist Short-staple Singles Ring Spun Yarns. *Textile Research Journal* 2007; 77, 9: 675-685.
19. Liu XJ, Su XZ, Wu TT. Effects of the Horizontal offset of the Ring Spinning Triangle on Yarn. *Fibres and Textiles in Eastern Europe* 2013; 21, 1: 35-40.
20. Su XZ, Gao WD, Liu XJ, Xie CP, Xu BJ. Theoretical Study of Yarn Torque Caused by Fibre Tension in the Spinning Triangle. *Fibres and Textiles in Eastern Europe* 2014; 22, 6(108): 41-50.

Received 14.04.2015 Reviewed 27.07.2015